HHS Public Access

Author manuscript

Brain Imaging Behav. Author manuscript; available in PMC 2016 June 01.

Published in final edited form as:

Brain Imaging Behav. 2015 June ; 9(2): 141–148. doi:10.1007/s11682-014-9291-2.

Gray & white matter tissue contrast differentiates MCI converters from non-converters

Angela L. Jefferson, PhD[a], **Katherine A. Gifford, PsyD**[a], **Stephen Damon**[a,*], **G. William Chapman IV**[a], **Dandan Liu, PhD**[d], **Jamie Sparling**[b], **Vitaly Dobromyslin**[c], **David Salat, PhD**[c,e,f], and **for the Alzheimer's Disease Neuroimaging Initiative**[**]

[a]Vanderbilt Memory & Alzheimer's Center, Department of Neurology, Vanderbilt University Medical Center, Nashville, TN, USA

[b]Boston University School of Medicine, Boston, MA, USA

[c]Neuroimaging Research for Veteran's Center, VA Boston Healthcare System, Boston, MA, USA

[d]Department of Biostatistics, Vanderbilt University; Nashville, TN, USA

[e]Athinoula A. Martinos Center for Biomedical Imaging, Charlestown, MA, USA

[f]Department of Radiology, Massachusetts General Hospital, Boston, MA, USA

Abstract

Objective—The clinical relevance of gray/white matter contrast ratio (GWR) in mild cognitive impairment (MCI) remains unknown. This study examined baseline GWR and 3-year follow-up diagnostic status in MCI.

Methods—Alzheimer's Disease Neuroimaging Initiative MCI participants with baseline 1.5T MRI and 3-year follow-up clinical data were included. Participants were categorized into two groups based on 3-year follow-up diagnoses: 1) non-converters (n=69, 75±7, 26% female), and 2) converters (i.e., dementia at follow-up; n=69, 75±7, 30% female) who were matched on baseline age and Mini-Mental State Examination scores. Groups were compared on FreeSurfer generated baseline GWR from structural images in which higher values represent greater tissue contrast.

Results—A general linear model, adjusting for APOE-status, scanner type, hippocampal volume, and cortical thickness, revealed that converters evidenced lower GWR values than non-converters (i.e., more degradation in tissue contrast; p=0.03).

Conclusions—Individuals with MCI who convert to dementia have lower baseline GWR values than individuals who remain diagnostically stable over a three-year period, statistically independent of cortical thickness or hippocampal volume.

[**]Data used in preparation of this article were obtained from the Alzheimer's Disease Neuroimaging Initiative (ADNI) database (adni.loni.ucla.edu). As such, the investigators within the ADNI contributed to the design and implementation of ADNI and/or provided data but did not participate in analysis or writing of this report. A complete listing of ADNI investigators can be found at: http://adni.loni.ucla.edu/wpcontent/uploads/how_to_apply/ADNI_Acknowledgement_List.pdf

Address Correspondence: Angela L. Jefferson, PhD, Vanderbilt Memory & Alzheimer's Center, 2525 West End Avenue, 12th Floor – Suite 1200, Nashville, TN 37203, Phone: 1-615-322-8676; Fax: 1-615-875-2727, angela.jefferson@vanderbilt.edu.

[*]completed statistical analysis

Keywords

Mild cognitive impairment; white matter; tissue contrast; imaging markers

Introduction

Individuals with mild cognitive impairment (MCI) have a higher propensity to develop dementia (Ganguli et al., 2011), so early identification is critical for primary and secondary intervention purposes. Recent diagnostic work-group recommendations request additional research identifying biomarkers, including structural imaging variables, for enhanced diagnostic accuracy (Albert et al., 2011). Tissue contrast is one potentially novel method to quantify early neuronal injury or microstructural changes in tissue properties. Gray to white matter signal intensity ratio (GWR) declines across the lifespan (Salat et al., 2009b). Furthermore, AD patients have more compromised GWR than cognitively normal elders (Westlye et al., 2009), and the spatial distribution of tissue contrast changes reflects regions associated with AD pathology, including the parahippocampal cortex (Salat et al., 2011). Thus, GWR may have potential as a unique neuroimaging marker of tissue loss and early neuropathological changes associated with unhealthy brain aging. That is, changes in tissue contrast may reflect a ratio of cell water and lipid content of gray and white tissue, taking into account the absolute signal variability across the brain as well as field inhomogeneities. However, the clinical significance of GWR in MCI is not yet known.

This study leverages a publically available dataset to examine the clinical implications of GWR by examining baseline gray matter/white matter tissue contrast in a cohort of MCI individuals who either convert or do not convert to dementia over a 3-year follow-up. In light of prior cross-sectional work showing that patients with AD have poor GWR relative to controls (Salat et al., 2011; Westlye et al., 2009), we hypothesized that tissue contrast would be poorer among participants with MCI at risk for conversion independent of neuroimaging markers of normal brain aging (i.e., cortical thickness, which cross-sectionally decreases across the cognitive aging spectrum (Lemaitre et al., 2012) and longitudinally decreases in community-based elders (Thambisetty et al., 2010)) and neurodegeneration (i.e., hippocampal volume (Killiany et al., 1993), one of the earliest neuroanatomical sites for AD-related neurodegeneration, especially in the CA1 stratum radiatum and stratum lacunosum-moleculare (Braak et al., 2006).

2. Material & Methods

2.1 Study Population

Participants were drawn from the Alzheimer's Disease Neuroimaging Initiative (ADNI; http://adni.loni.ucla.edu/) launched in 2004. The original ADNI study enrolled approximately 800 participants, aged 55–90 years. ADNI exclusion criteria included serious neurological disease other than AD, history of brain lesion or head trauma, and history of psychoactive medication use (for full inclusion/exclusion criteria please refer to http://www.adni-info.org). Analysis of ADNI's publically available database was approved by our local Institutional Review Boards prior to data access or analysis.

The current study included individuals with a baseline diagnosis of MCI who had a baseline Mini-Mental State Examination (MMSE) score, maintained enrollment in ADNI for at least 36 months, and had a 36-month follow-up diagnosis of MCI or dementia. These criteria resulted in a pool of 211 participants, which was divided into two groups: 1) converters or participants with dementia (McKhann et al., 1984) at their 36-month follow-up visit and 2) non-converters or participants who remained MCI. These groups were then matched for age and MMSE score (Hulley, 2001; Thomas and Greenland, 1983) by filtering the subset of non-converters for age and then making a one-to-one match (i.e., converter to non-converter) on age and MMSE score. This process resulted in a sample of 138 MCI participants (n=69 converters, n=69 nonconverters). APOE genotyping was performed by the ADNI Biomarker Core (see http://www.adni-info.org/).

2.2 Neuroimaging scan acquisition & analysis

The ADNI neuroimaging protocol has been reported in detail (Jack et al., 2008; Weiner et al., 2010). For the current study, the raw 1.5T MRI T1-weighted sagittal volumetric magnetization prepared rapid gradient echo sequence high resolution structural images (1.25mm×1.25mm×1.20mm) were downloaded from ADNI's publically available neuroimaging online databank (http://www.loni.ucla.edu/ADNI/Data/index.shtml). Before processing, all scans were viewed on a slice-by-slice basis to confirm motion and other artifacts were not present. Images were post-processed using FreeSurfer (http://surfer.nmr.mgh.harvard.edu/) (Dale et al., 1999; Fischl et al., 1999). Subject data were run through the reconstruction process for skull stripping, intensity normalization, and surface segmentation. Manual intervention to correct for registration, topological, and segmentation defects were included during post-processing. White and gray surfaces were manually inspected and corrected in accordance with the FreeSurfer manual (i.e., http://surfer.nmr.mgh.harvard.edu/fswiki/Edits). After manual intervention, images were re-processed through FreeSurfer to update the transformation template and segmentation information. Per FreeSurfer algorithms, the gray/white matter boundary was computed to serve as a reference for custom-defined surfaces. After surface generation, all surfaces were smoothed at 30mm full-width/half-maximum Gaussian kernel to reduce the effects of noise on the results (Salat et al., 2009a; Salat et al., 2009b). Three measures of interest were derived using FreeSurfer:

1. GWR: As described previously (Salat et al., 2011; Salat et al., 2009b), images were corrected using a highly localized (to within 2mm) nonparametric, nonuniform intensity normalization procedure to correct for inhomogeneity prior to sampling gray and white matter tissue intensity (Sled et al., 1998). Gray matter signal intensity was measured at a depth of 35% of the cortical ribbon thickness beginning from the gray matter/white matter border and projecting toward the gray matter/CSF border. White matter signal intensity was measured at 1mm subjacent to the gray matter/white matter border. The GWR surface was then constructed with lower values indicating less distinct intensities (see Figure 1 for illustration). The GWR measurement was numerically calculated as 100*(white matter intensity–gray matter intensity)/(white matter intensity+gray matter intensity).

2. Hippocampal volume: Images underwent automated segmentation (Fischl et al., 2004). Regional volume was calculated based upon the number of voxels occupied within the region of interest. Hippocampal volume was then corrected for intracranial volume (ICV) defined by FreeSurfer's automated method (Buckner et al., 2004). MPRAGE images were intensity normalized then segmented into CSF, gray, or white matter. Contiguous regions were detected based on intensity similarity and spatial gradient (contour). Bias fields were modeled as a three-dimensional second order polynomial. After three iterations of likelihood maximizations of the hidden Markov random field model, the estimated total intracranial volume (etICV) was computed as the sum of the gray and white matter voxels. ICV-corrected hippocampal volumes was computed as hippocampal volume/etICV*100.

3. Cortical thickness: Both intensity and continuity information were used to produce representations of cortical thickness, calculated as the closest difference from the gray/white matter boundary to the gray matter/CSF boundary at each surface vertex (Fischl and Dale, 2000). The generated maps relied on spatial intensity gradients not restricted to the voxel resolution, so they were not affected by absolute signal intensity and were able to detect submillimeter features. Such cortical thickness procedures have been validated with histological (Rosas et al., 2002) and manual measurements (Salat et al., 2004).

2.3 Statistical analyses

For hypothesis testing, GWR was analyzed with a vertex-by-vertex general linear model (GLM) between conversion groups adjusting for apolipoprotein ε4 (APOE4) carrier status (i.e., positive defined as e2/e4, e3/e4, e4/e4 versus negative defined as e2/e2, e2/e3, e3/e3 (Yip et al., 2005)), scanner type (Han et al., 2006), cortical thickness (i.e., a marker of brain aging (Risacher et al., 2009)), and hippocampal volume (i.e., a marker of neurodegeneration (Braak et al., 2006)). To assess the stability of our observations, a Monte Carlo simulation technique was applied using 5000 iterations of repeated random sampling. The simulation models related GWR to conversion status, adjusting for APOE4 status, scanner type, and hippocampal volume. Cortical thickness was excluded in the simulation models because the technique implemented does not allow for the inclusion of a per-vertex regressor. MMSE and age were not included as covariates, as the groups were matched *a priori* on these factors.

As a secondary analysis, hierarchical models were used to compare goodness-of-fits between models. One neuroimaging marker (marker A) was related to conversion status, and we tested the incremental deviance value (i.e., a likelihood ratio-based test statistic for multivariate logistic regression) of adding a second neuroimaging marker (marker B) to the model. Next, we tested the incremental deviance value of adding the remaining neuroimaging marker (marker C) to the previous model. Six sets of hierarchical models were run, representing each possible permutation for ordering the three neuroimaging variables (i.e., ABC, BAC, BCA, CBA, CAB, ACB; where A=hippocampal volume, B=cortical thickness, and C=GWR). Significance thresholding was set for all analyses at $p<0.05$. Analyses were conducted using SPSS 19.0 and MATLAB R2012a.

3. Results

3.1 Participant Characteristics

Converters and non-converters differed for APOE status (χ^2=5.7, p=0.017), ICV-corrected hippocampal volume (F=11.71, p<0.001), cortical thickness (F=3.89, p=.05), 36-month follow-up MMSE score (F=38.3, p<0.001), baseline Logical Memory Delayed Recall (F=16.0, p<0.001) and 36-month Logical Memory Delayed Recall (F=42.3, p<0.001). However, the two groups did not differ for education (F=1.21, p=0.27), sex (χ^2=0.32, p=0.57), race (χ^2=0.34, p=0.84), global white matter intensity (F=1.59, p=0.14), or global gray matter intensity (F=2.32, p=0.06). See Table 1 for details.

3.2 Imaging Comparisons

Unadjusted correlation coefficients for the entire sample (n=138) yielded associations between GWR and cortical thickness (left hemisphere r=0.71, p<0.001; right hemisphere=0.72, p<0.001) and cortical thickness and ICV-corrected hippocampal volume (left hemisphere r=0.31, p<0.001; right hemisphere=0.43, p<0.001). However associations were not observed for GWR and ICV-corrected hippocampal volume (left hemisphere r=0.03, p=0.65; right hemisphere r=0.03, p=0.70).

3.3 Baseline GWR & Conversion Status

In a model adjusting for baseline hippocampal volume, baseline per-vertex cortical thickness, scanner type, and APOE4 status, converters evidenced regions with significantly lower baseline global GWR values as compared to non-converters (F=3.21, p=0.03). Regions where GWR differences were observed between the two groups include areas within the bilateral middle temporal lobe, left superior temporal lobe, bilateral subparietal region, left calcarine, and left precuneus (Figure 2a). Results were similar when the original, unsmoothed images were used to regenerate the surfaces (data not shown). Results were also similar based on the Monte Carlo simulations (see Figure 2b).

3.4. Secondary Multivariate Logistic Regression Analyses

Results from multivariate logistic regression are presented in Table 2. For Model set 1, (i.e., hippocampal volume, cortical thickness, and GWR in that order) there was no improvement in model fits when cortical thickness was added in the model with hippocampal volume (p=0.21); however, when GWR was added, there was a significant improvement (p=0.047). Model set 2 switched the order of variable entry between GWR and cortical thickness (i.e., hippocampal volume, GWR, and cortical thickness in that order) with similar results. When GWR was added to hippocampal volume, the model had a better fit (p=0.025); however, no improvement was found when cortical thickness was added.

Model set 3 (i.e., cortical thickness, GWR, and hippocampal volume in that order) resulted in significant improvement of model fits when GWR (p=0.02) and hippocampal volume (p=0.0008) were added to the model hierarchically. Model set 4 switched the order of variable entry between GWR and hippocampal volume (i.e., cortical thickness, hippocampal volume, and GWR) with similar results. The improvement of model fit was significant when

hippocampal volume (p=0.0004) and GWR (p=0.047) were added to cortical thickness hierarchically.

Model set 5 (i.e., in order, GWR, cortical thickness and hippocampal volume) resulted in no improvement in model fits when cortical thickness was added to GWR in the model (p=0.92); however, when hippocampal volume was added to the previous model, there was a significant improvement (p=0.0008). Model set 6 switched the order of variable entry between cortical thickness and hippocampal volume (i.e., in order, GWR, hippocampal volume, cortical thickness) with similar results. When hippocampal volume was added to GWR, there was a better model fit (p=0.001), but no improvement was observed when cortical thickness was added (p=0.49). In summary, across all six models, GWR and hippocampal volume consistently improve model fit while cortical thickness does not improve model fit.

4. Discussion

Leveraging a national, publically available dataset, the current study found that individuals with MCI who later convert to dementia have poorer gray matter/white matter tissue contrast at baseline than a cohort of MCI individuals who remain stable over the 3-year follow-up period. The observed tissue contrast difference is particularly noteworthy for several reasons. First, GWR differences occurred in light of no between-group statistical differences in global white matter tissue intensity and a non-significant trend for global gray matter tissue intensity differences. Second, the GWR differences were statistically independent of APOE4 status and two conventional neuroimaging markers (i.e., cortical thickness (Lemaitre et al., 2012; Thambisetty et al., 2010) and ICV-corrected hippocampal volume (Braak et al., 2006; Killiany et al., 1993)). Third, findings appear relatively stable as demonstrated by the simulation results. Finally, when statistically considering the GWR variable in multivariate models with the two conventional neuroimaging markers (i.e., cortical thickness and ICV-corrected hippocampal volume), GWR and ICV-corrected hippocampal volume were consistently predictive of conversion outcome while cortical thickness was not. Therefore, it appears GWR may offer unique information regarding neuroanatomical changes linked to increased risk for conversion to dementia.

Prior studies have examined tissue contrast in aging (Magnaldi et al., 1993; Salat et al., 2009b), AD (Salat et al., 2011), schizophrenia (Kong et al., 2012), and epilepsy (Thesen et al., 2011). For example, over two decades ago, Raz and colleagues (1990) observed a change in the differentiation of gray and white matter on T1 imaging, and this tissue contrast difference was related to cognition among a small cohort (n=26) of older adults. Using a subjective rating scale, Magnaldi et al. (1993), reported significantly decreased regional contrast between gray and white matter in adults in the sixth and seventh decade relative to those adults in the third decade of life. These age-related differences were later replicated by Salat et al (2009b), and extended to include regional measurements of GWR using the same FreeSurfer method implemented in the current study (Salat et al., 2009a). GWR as quantified by FreeSurfer also differs in patients with AD (Salat et al., 2009a) relative to controls when adjusting for cortical thickness, schizophrenia relative to controls when

adjusting for cortical thickness (Kong et al., 2012), and epilepsy relative to controls (Thesen et al., 2011), albeit with different anatomical patterns.

There is a strong need for early diagnosis of AD in the MCI or preclinical stages, with recent recommendations calling for identifying biomarkers, such as structural imaging changes, of underlying AD pathophysiology (Jack et al., 2010). The current findings extend prior work examining tissue contrast in normal (Magnaldi et al., 1993) and abnormal brain aging (Kong et al., 2012; Salat et al., 2011) by highlighting the clinical significance of GWR in longitudinal outcomes among older adults "at risk" for dementia. That is, even when statistically considering key imaging (hippocampal volume, cortical thickness) and genetic risk factors (APOE4) associated with cognitive decline, GWR was more compromised at baseline among MCI participants who converted to dementia over the 3-year follow-up period. GWR may be a particularly valuable imaging marker in MCI (and perhaps even pre-MCI) for detecting microstructural changes in the signal intensity between gray and white matter tissue and aiding in identification of individuals at risk for AD. Future research will need to examine the clinical relevance of GWR in the pre-MCI phase.

It is noteworthy that the observed effects in tissue contrast between the converter and non-converter MCI groups were predominantly detected in the left hemisphere. That is, in the adjusted models, significant differences were observed in the bilateral middle temporal lobe, left superior temporal lobe, bilateral subparietal region, left calcarine, and left precuneus. Many of these regions, such as the middle temporal lobe (Beckett et al., 2012), superior temporal lobe (Arnold et al., 1991; Beckett et al., 2012; Wu et al., 2012), and left precuneus (Baron et al., 2001; Sperling et al., 2009; Wu et al., 2012), are directly implicated early in the AD pathological process. Furthermore, prior studies have linked hypometabolism in the precuneus to clinical memory dysfunction (Herholz et al., 2002). The laterality of our observations may also be attributable to the enrollment criteria applied to this specific cohort, which emphasized a verbal amnestic neuropsychological profile defined by impairments on paragraph learning (Petersen et al., 2010). Verbal episodic memory performances are mediated by left hemisphere structures, which may contribute to more lateral effects.

The underlying pathological mechanism for the reduction in contrast is not well understood. Changes in white matter signal intensity can occur as a function of increased water content with myelin structural changes (Blackmon et al., 2011), small vessel disease resulting in white matter changes (van Norden et al., 2011), or astrocytic gliosis (Kitagaki et al., 1997). In contrast, gray matter signal intensity changes are generally due to neuronal loss (Rusinek et al., 1991). The contrast values in the current study were calculated using T1 images, which relate cell water and lipid content of gray and white tissue. Therefore, reductions in tissue contrast ratio may be due to an increased gray matter signal resulting from decreased water content and a decreased white matter signal due to demyelination. A ratio between tissue types may offer a measure that takes into account absolute signal variability across the brain as well as field inhomogeneities.

The current study has a number of strengths. First, we assessed GWR, a relatively unique measure of gray and white matter structural integrity. We expand prior work (Salat et al.,

2011) by assessing the clinical relevance of GWR in a sample of individuals at risk for dementia. Additionally, individuals in this sample were matched for baseline cognitive status (MMSE) and age and did not differ with respect to other key demographic variables. The ADNI data offers a number of strengths, including nationwide representation of participants, standardized neuroimaging protocol, and standardized diagnostic criteria.

Despite these strengths, participants comprising the ADNI dataset are predominantly White and well-educated (i.e., with a mean education of 16 years). Additionally, ADNI is a cohort study and was designed to support research aimed at discovery and treatment development, which may limit the generalizability of findings. Though we focused on GWR while statistically holding constant the effects of cortical thickness and hippocampal volume, it is important to highlight the multicollinearity of neuroimaging variables as a common limitation in cognitive aging research. As an example, the calculation of GWR includes measuring the depth of 35% of the cortical ribbon from the gray matter/white matter border. GWR and cortical thickness are not entirely independent of one another, an observation supported in our study by significant bilateral unadjusted correlation values. While the current results focus on baseline neuroimaging markers in relation to 3-year follow-up conversion status, the design is still cross-sectional in nature. Longitudinal studies are needed to model GWR changes over time and determine how such change affects disease progression. The current study results do not reconcile the underlying etiology associated with GWR compromise, including the mechanism(s) or pathophysiological process(es) behind degradation in tissue contrast. Additional research is needed to better understand the etiology of GWR changes.

5. Conclusions

This study found that individuals with MCI who later convert to dementia have poorer gray matter/white matter tissue contrast at baseline than a cohort of MCI individuals who remain stable over the 3-year follow-up period. The observed tissue contrast difference occurred despite no between-group statistical differences in global gray matter tissue intensity or white matter tissue intensity and was statistically independent of APOE4 status, cortical thickness, and hippocampal volume. Future studies are needed to model GWR changes over time to determine how changes in tissue contrast affect disease progression as well as the underlying etiology associated with GWR compromise.

Acknowledgements

This research was supported by K23-AG030962 (Paul B. Beeson Career Development Award in Aging; ALJ); Alzheimer’s Association IIRG-08-88733 (ALJ); R01-AG034962 (ALJ); R01-HL111516 (ALJ); K24-AG046373 (ALJ); American Federation for Aging Research Medical Student Training in Aging Research Grant (JS; T35-AG038027); R01-NR010827 (DS); and the Vanderbilt Memory & Alzheimer’s Center. Data collection and sharing for this project was funded by the Alzheimer's Disease Neuroimaging Initiative (ADNI) (National Institutes of Health Grant U01 AG024904). ADNI is funded by the National Institute on Aging, by the National Institute of Biomedical Imaging and Bioengineering, and through generous contributions from the following: Abbott; Alzheimer’s Association; Alzheimer’s Drug Discovery Foundation; Amorfix Life Sciences Ltd.; AstraZeneca; Bayer HealthCare; BioClinica, Inc.; Biogen Idec, Inc.; Bristol-Myers Squibb Company; Eisai, Inc.; Elan Pharmaceuticals, Inc.; Eli Lilly and Company; F. Hoffmann-La Roche Ltd. and its affiliated company Genentech, Inc.; GE Healthcare; Innogenetics, N.V.; IXICO Ltd.; Janssen Alzheimer Immunotherapy Research & Development, LLC.; Johnson & Johnson Pharmaceutical Research & Development, LLC.; Medpace, Inc.; Merck & Co., Inc.; Meso Scale Diagnostics, LLC.; Novartis Pharmaceuticals Corporation; Pfizer, Inc.; Servier; Synarc, Inc.;

and Takeda Pharmaceutical Company. The Canadian Institutes of Health Research is providing funds to support ADNI clinical sites in Canada. Private sector contributions are facilitated by the Foundation for the National Institutes of Health (www.fnih.org). The grantee organization is the Northern California Institute for Research and Education, and the study is coordinated by the Alzheimer's Disease Cooperative Study Rev October 16, 2012 at the University of California, San Diego. ADNI data are disseminated by the Laboratory for Neuro Imaging at the University of California, Los Angeles. This research was also supported by NIH grants P30 AG010129 and K01 AG030514.

References

Albert MS, Dekosky ST, Dickson D, Dubois B, Feldman HH, Fox NC, Gamst A, Holtzman DM, Jagust WJ, Petersen RC, Snyder PJ, Carrillo MC, Thies B, Phelps CH. The diagnosis of mild cognitive impairment due to Alzheimer's disease: Recommendations from the National Institute on Aging-Alzheimer's Association workgroups on diagnostic guidelines for Alzheimer's disease. Alzheimers Dement. 2011; 7:270–279. [PubMed: 21514249]

Arnold SE, Hyman BT, Flory J, Damasio AR, Van Hoesen GW. The topographical and neuroanatomical distribution of neurofibrillary tangles and neuritic plaques in the cerebral cortex in patients with Alzheimer's disease. Cerebral Cortex. 1991; 1:103–116. [PubMed: 1822725]

Baron JC, Chetelat G, Desgranges B, Perchey G, Landeau B, de la Sayette V, Eustache F. In vivo mapping of gray matter loss with voxel-based morphometry in mild Alzheimer's disease. Neuroimage. 2001; 14:298–309. [PubMed: 11467904]

Beckett TL, Webb RL, Niedowicz DM, Holler CJ, Matveev S, Baig I, LeVine H 3rd, Keller JN, Murphy MP. Postmortem Pittsburgh Compound B (PiB) binding increases with Alzheimer's disease progression. Journal of Alzheimer's Disease. 2012; 32:127–138.

Blackmon K, Halgren E, Barr WB, Carlson C, Devinsky O, DuBois J, Quinn BT, French J, Kuzniecky R, Thesen T. Individual differences in verbal abilities associated with regional blurring of the left gray and white matter boundary. The Journal of Neuroscience. 2011; 31:15257–15263. [PubMed: 22031871]

Braak H, Alafuzoff I, Arzberger T, Kretzschmar H, Del Tredici K. Staging of Alzheimer disease-associated neurofibrillary pathology using paraffin sections and immunocytochemistry. Acta Neuropathol. 2006; 112:389–404. [PubMed: 16906426]

Buckner RL, Head D, Parker J, Fotenos AF, Marcus D, Morris JC, Snyder AZ. A unified approach for morphometric and functional data analysis in young old, and demented adults using automated atlas-based head size normalization: Reliability and validation against manual measurement of total intracranial volume. Neuroimage. 2004; 23:724–738. [PubMed: 15488422]

Dale AM, Fischl B, Sereno MI. Cortical surface-based analysis: I. Segmentation and surface reconstruction. Neuroimage. 1999; 9:179–194. [PubMed: 9931268]

Fischl B, Dale AM. Measuring the thickness of the human cerebral cortex from magnetic resonance images. Proc Natl Acad Sci U S A. 2000; 97:11050–11055. [PubMed: 10984517]

Fischl B, Salat DH, van der Kouwe AJ, Makris N, Segonne F, Quinn BT, Dale AM. Sequence-independent segmentation of magnetic resonance images. Neuroimage. 2004; 23(Suppl 1):S69–S84. [PubMed: 15501102]

Fischl B, Sereno MI, Tootell RB, Dale AM. High-resolution intersubject averaging and a coordinate system for the cortical surface. Human Brain Mapping. 1999; 8:272–284. [PubMed: 10619420]

Ganguli M, Snitz BE, Saxton JA, Chang CC, Lee CW, Vander Bilt J, Hughes TF, Loewenstein DA, Unverzagt FW, Petersen RC. Outcomes of mild cognitive impairment by definition: A population study. Archives of Neurology. 2011; 68:761–767. [PubMed: 21670400]

Han X, Jovicich J, Salat D, van der Kouwe A, Quinn B, Czanner S, Busa E, Pacheco J, Albert M, Killiany R, Maguire P, Rosas D, Makris N, Dale A, Dickerson B, Fischl B. Reliability of MRI-derived measurements of human cerebral cortical thickness: The effects of field strength, scanner upgrade and manufacturer. Neuroimage. 2006; 32:180–194. [PubMed: 16651008]

Herholz K, Salmon E, Perani D, Baron JC, Holthoff V, Frolich L, Schonknecht P, Ito K, Mielke R, Kalbe E, Zundorf G, Delbeuck X, Pelati O, Anchisi D, Fazio F, Kerrouche N, Desgranges B, Eustache F, Beuthien-Baumann B, Menzel C, Schroder J, Kato T, Arahata Y, Henze M, Heiss WD. Discrimination between Alzheimer dementia and controls by automated analysis of multicenter FDG PET. Neuroimage. 2002; 17:302–316. [PubMed: 12482085]

Hulley, SB.; Cummings, SR.; Browner, WS.; Grady, DG.; Newman, TB. Designing Clinical Research. Philadelphia, PA: Lippincott Williams & Wilkins; 2001.

Jack CR Jr, Bernstein MA, Fox NC, Thompson P, Alexander G, Harvey D, Borowski B, Britson PJ, J LW, Ward C, Dale AM, Felmlee JP, Gunter JL, Hill DL, Killiany R, Schuff N, Fox-Bosetti S, Lin C, Studholme C, DeCarli CS, Krueger G, Ward HA, Metzger GJ, Scott KT, Mallozzi R, Blezek D, Levy J, Debbins JP, Fleisher AS, Albert M, Green R, Bartzokis G, Glover G, Mugler J, Weiner MW. The Alzheimer's Disease Neuroimaging Initiative (ADNI): MRI methods. Journal of Magnetic Resonance Imaging. 2008; 27:685–691. [PubMed: 18302232]

Jack CR Jr, Knopman DS, Jagust WJ, Shaw LM, Aisen PS, Weiner MW, Petersen RC, Trojanowski JQ. Hypothetical model of dynamic biomarkers of the Alzheimer's pathological cascade. Lancet Neurol. 2010; 9:119–128. [PubMed: 20083042]

Killiany RJ, Moss MB, Albert MS, Sandor T, Tieman J, Jolesz F. Temporal lobe regions on magnetic resonance imaging identify patients with early Alzheimer's disease. Archives of Neurology. 1993; 50:949–954. [PubMed: 8363449]

Kitagaki H, Mori E, Hirono N, Ikejiri Y, Ishii K, Imamura T, Ikeda M, Yamaji S, Yamashita H, Shimomura T, Nakagawa Y. Alteration of white matter MR signal intensity in frontotemporal dementia. American Journal of Neuroradiology. 1997; 18:367–378. [PubMed: 9111678]

Kong L, Herold C, Stieltjes B, Essig M, Seidl U, Wolf RC, Wustenberg T, Lasser MM, Schmid LA, Schnell K, Hirjak D, Thomann PA. Reduced gray to white matter tissue intensity contrast in schizophrenia. PLoS One. 2012; 7:e37016. [PubMed: 22615876]

Lemaitre H, Goldman AL, Sambataro F, Verchinski BA, Meyer-Lindenberg A, Weinberger DR, Mattay VS. Normal age-related brain morphometric changes: Nonuniformity across cortical thickness, surface area and gray matter volume? Neurobiology Aging. 2012; 33:617 e611–619 e611.

Magnaldi S, Ukmar M, Vasciaveo A, Longo R, Pozzi-Mucelli RS. Contrast between white and grey matter: MRI appearance with ageing. European Radiology. 1993; 3:513–519.

McKhann G, Drachman D, Folstein M, Katzman R, Price D, Stadlan EM. Clinical diagnosis of Alzheimer's disease: report of the NINCDS-ADRDA Work Group under the auspices of Department of Health and Human Services Task Force on Alzheimer's Disease. Neurology. 1984; 34:939–944. [PubMed: 6610841]

Petersen RC, Aisen PS, Beckett LA, Donohue MC, Gamst AC, Harvey DJ, Jack CR Jr, Jagust WJ, Shaw LM, Toga AW, Trojanowski JQ, Weiner MW. Alzheimer's Disease Neuroimaging Initiative (ADNI): Clinical characterization. Neurology. 2010; 74:201–209. [PubMed: 20042704]

Raz N, Millman D, Sarpel G. Cerebral correlates of cognitive aging: Gray-white-matter differentiation in the medial temporal lobes, and fluid versus crystallized abilities. Psychobiology. 1990; 18:475–481.

Risacher SL, Saykin AJ, West JD, Shen L, Firpi HA, McDonald BC. Baseline MRI predictors of conversion from MCI to probable AD in the ADNI cohort. Current Alzheimer Research. 2009; 6:347–361. [PubMed: 19689234]

Rosas HD, Liu AK, Hersch S, Glessner M, Ferrante RJ, Salat DH, van der Kouwe A, Jenkins BG, Dale AM, Fischl B. Regional and progressive thinning of the cortical ribbon in Huntington's disease. Neurology. 2002; 58:695–701. [PubMed: 11889230]

Rusinek H, de Leon MJ, George AE, Stylopoulos LA, Chandra R, Smith G, Rand T, Mourino M, Kowalski H. Alzheimer disease: Measuring loss of cerebral gray matter with MR imaging. Radiology. 1991; 178:109–114. [PubMed: 1984287]

Salat DH, Buckner RL, Snyder AZ, Greve DN, Desikan RS, Busa E, Morris JC, Dale AM, Fischl B. Thinning of the cerebral cortex in aging. Cerebral Cortex. 2004; 14:721–730. [PubMed: 15054051]

Salat DH, Chen JJ, van der Kouwe AJ, Greve DN, Fischl B, Rosas HD. Hippocampal degeneration is associated with temporal and limbic gray matter/white matter tissue contrast in Alzheimer's disease. Neuroimage. 2011; 54:1795–1802. [PubMed: 20965261]

Salat DH, Greve DN, Pacheco JL, Quinn BT, Helmer KG, Buckner RL, Fischl B. Regional white matter volume differences in nondemented aging and Alzheimer's disease. Neuroimage. 2009a; 44:1247–1258. [PubMed: 19027860]

Salat DH, Lee SY, van der Kouwe AJ, Greve DN, Fischl B, Rosas HD. Age-associated alterations in cortical gray and white matter signal intensity and gray to white matter contrast. Neuroimage. 2009b; 48:21–28. [PubMed: 19580876]

Sled JG, Zijdenbos AP, Evans AC. A nonparametric method for automatic correction of intensity nonuniformity in MRI data. IEEE Transactions on Medical Imaging. 1998; 17:87–97. [PubMed: 9617910]

Sperling RA, Laviolette PS, O'Keefe K, O'Brien J, Rentz DM, Pihlajamaki M, Marshall G, Hyman BT, Selkoe DJ, Hedden T, Buckner RL, Becker JA, Johnson KA. Amyloid deposition is associated with impaired default network function in older persons without dementia. Neuron. 2009; 63:178–188. [PubMed: 19640477]

Thambisetty M, Wan J, Carass A, An Y, Prince JL, Resnick SM. Longitudinal changes in cortical thickness associated with normal aging. Neuroimage. 2010; 52:1215–1223. [PubMed: 20441796]

Thesen T, Quinn BT, Carlson C, Devinsky O, DuBois J, McDonald CR, French J, Leventer R, Felsovalyi O, Wang X, Halgren E, Kuzniecky R. Detection of epileptogenic cortical malformations with surface-based MRI morphometry. PLoS One. 2011; 6:e16430. [PubMed: 21326599]

Thomas DC, Greenland S. The relative efficiencies of matched and independent sample designs for case-control studies. J Chronic Dis. 1983; 36:685–697. [PubMed: 6630405]

van Norden AG, de Laat KF, Gons RA, van Uden IW, van Dijk EJ, van Oudheusden LJ, Esselink RA, Bloem BR, van Engelen BG, Zwarts MJ, Tendolkar I, Olde-Rikkert MG, van der Vlugt MJ, Zwiers MP, Norris DG, de Leeuw FE. Causes and consequences of cerebral small vessel disease. The RUN DMC study: A prospective cohort study. Study rationale and protocol. BMC Neurol. 2011; 11:29. [PubMed: 21356112]

Weiner MW, Aisen PS, Jack CR Jr, Jagust WJ, Trojanowski JQ, Shaw L, Saykin AJ, Morris JC, Cairns N, Beckett LA, Toga A, Green R, Walter S, Soares H, Snyder P, Siemers E, Potter W, Cole PE, Schmidt M. The Alzheimer's disease neuroimaging initiative: Progress report and future plans. Alzheimers Dement. 2010; 6:202 e207–211 e207. [PubMed: 20451868]

Westlye LT, Walhovd KB, Dale AM, Espeseth T, Reinvang I, Raz N, Agartz I, Greve DN, Fischl B, Fjell AM. Increased sensitivity to effects of normal aging and Alzheimer's disease on cortical thickness by adjustment for local variability in gray/white contrast: a multi-sample MRI study. Neuroimage. 2009; 47:1545–1557. [PubMed: 19501655]

Wu L, Rowley J, Mohades S, Leuzy A, Dauar MT, Shin M, Fonov V, Jia J, Gauthier S, Rosa-Neto P. Alzheimer's Disease Neuroimaging, I. Dissociation between brain amyloid deposition and metabolism in early mild cognitive impairment. PLoS One. 2012; 7:e47905. [PubMed: 23112868]

Yip AG, McKee AC, Green RC, Wells J, Young H, Cupples LA, Farrer LA. APOE, vascular pathology, and the AD brain. Neurology. 2005; 65:259–265. [PubMed: 16043796]

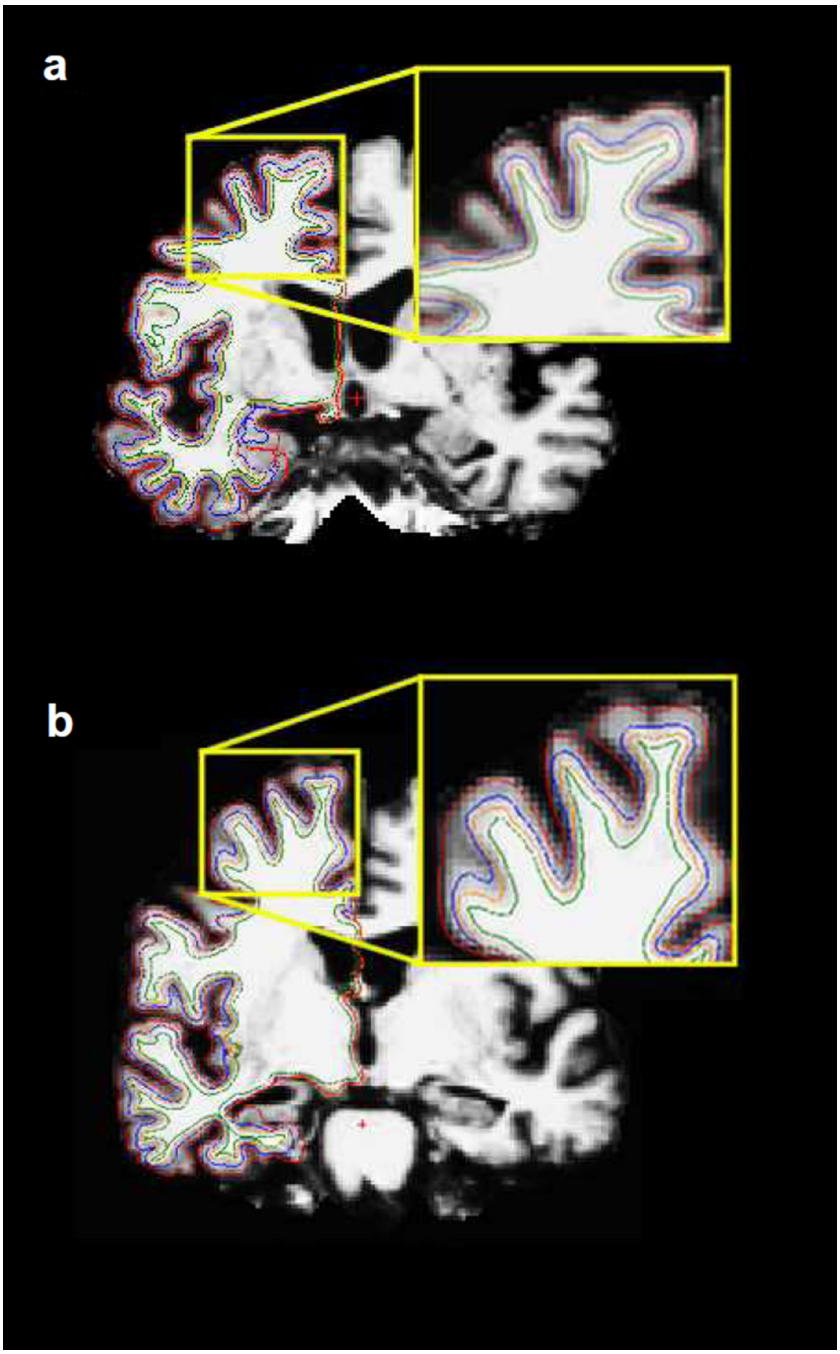

Figure 1. Illustration of GWR Protocol

(**a**) Non-converter (76 year old man, MMSE=24) and (**b**) Converter (76 year old man, MMSE=24). Orange line=gray/white boundary; green line=white matter surface, generated 1mm below the gray/white boundary; red line=outer pial surface; blue line=gray matter surface, generated 35% of the way from gray/white boundary to pial outer boundary.

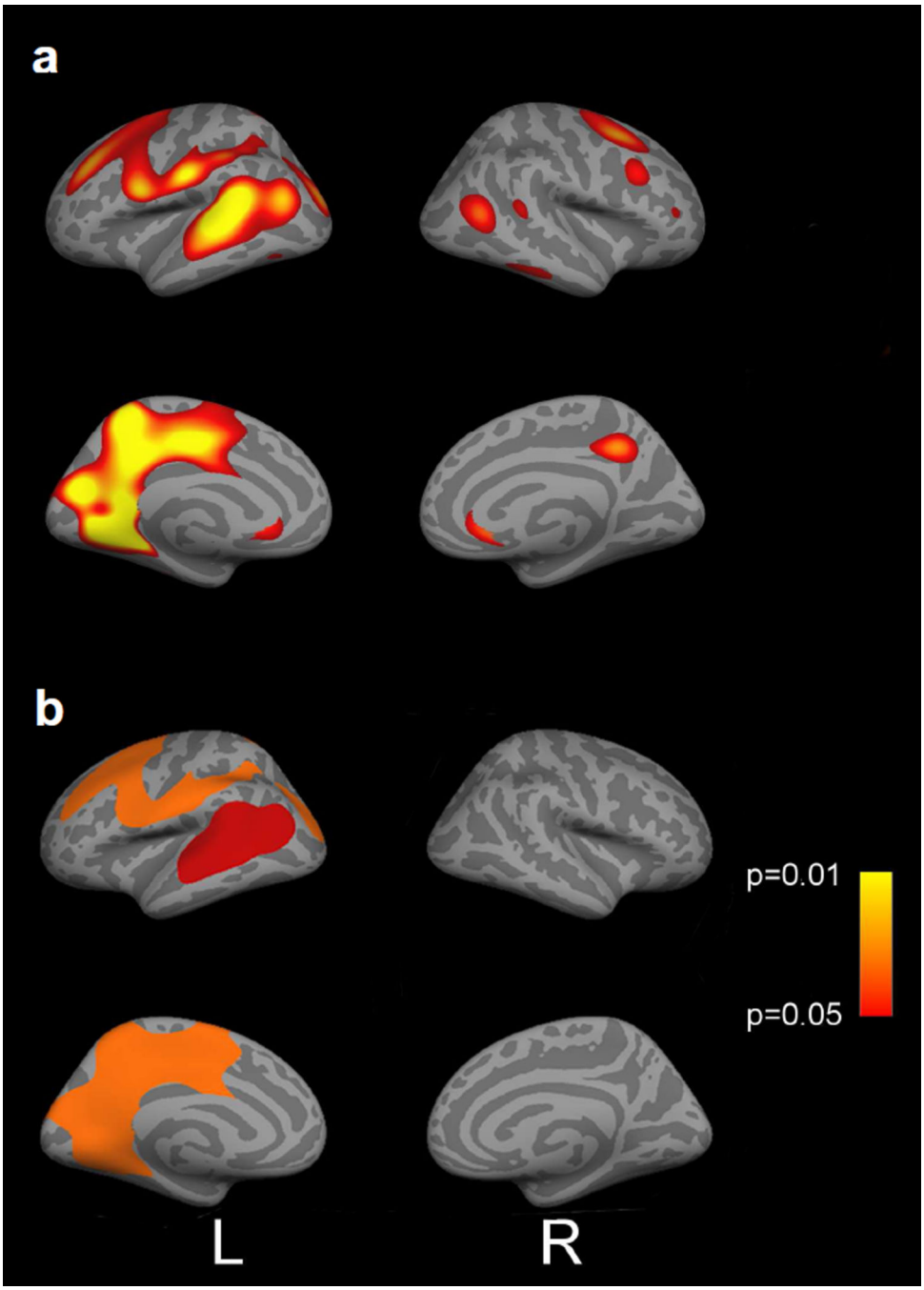

Figure 2. GWR Differences for Converters and Non-converters

Top images in each panel represent lateral view. **Panel a:** Converters showed areas of lower GWR compared to non-converters when the model adjusted for scanner type, APOE4 status, ICV-corrected hippocampal volume and cortical thickness. **Panel b:** GWR differences when comparing converters to non-converters corrected for multiple comparisons by running n iterations of Monte Carlo simulations with a cluster-wise and vertex-wise threshold of

$p<0.05$ where converters showed areas of lower GWR compared to non-converters when the model adjusted for scanner type, APOE4 status, and ICV-corrected hippocampal volume.

Table 1

Participant Characteristics

	Non-converters n=69	Converters n=69
Age, years	75±7	75±7
Sex, % female	26	30
Race, % White	91	93
Education, years	16±3	17±3
APOE4, % carrier	43%	64%
Baseline MMSE	27±2	27±2
36-month MMSE*	26±5	21±5
Baseline Logical Memory Delayed Recall*	4.5±2.6	2.8±2.4
36-month Logical Memory Delayed Recall*	6.0±5.5	1.1±2.4
Baseline ICV-corrected hippocampal volume**	0.42±0.08	0.38±0.06
Cortical thickness	2.12±0.12	2.08±0.13
Gray matter intensity	73.8±2.3	74.0±2.1
White matter intensity	103.9±0.9	103.8±1.1
GWR*	27.2±2.1	26.5±1.6

Note. Data presented as M±SD or percentage; MMSE=Mini-Mental State Examination; ICV=intracranial volume corrected;

* =p<0.01 difference between groups;

** =p<0.001 difference between groups

Table 2

Multivariate Model Results

Model Set	Variables	Difference in deviance*	p-value†
1	ICV-corrected hippocampal volume	--	--
	Cortical thickness	1.52	0.21
	GWR	3.93	0.047
2	ICV-corrected hippocampal volume	--	--
	GWR	4.97	0.025
	Cortical thickness	0.48	0.487
3	Cortical thickness	--	--
	GWR	5.18	0.022
	ICV-corrected hippocampal volume	11.25	0.0008
4	Cortical thickness	--	--
	ICV-corrected hippocampal volume	12.50	0.0004
	GWR	3.93	0.047
5	GWR	--	--
	Cortical thickness	0.01	0.92
	ICV-corrected hippocampal volume	11.25	0.0008
6	GWR	--	--
	ICV-corrected hippocampal volume	10.79	0.001
	Cortical thickness	0.48	0.487

Note.

*=deviance is defined as minus 2 times the maximum log-likelihood generated from the model;

†=represents the statistical significance for the difference in deviance when a new neuroimaging marker is added to the model in the prediction of conversion status.